Korean J. Chem. Eng., **30**(5), 1142-1152 (2013)
DOI: 10.1007/s11814-013-0031-x

Fabrication of superhydrophobic surfaces using structured colloids

Young-Sang Cho*,†, Jong Woo Moon, Dong Chan Lim***, and Young Dok Kim******

*Department of Chemical Engineering and Biotechnology, Korea Polytechnic University, 237, Siheung-si, Gyeonggi-do 429-793, Korea
**Division of Powder and Ceramics, Korea Institute of Materials Science, 66, Sangnam-dong, Changwon, Gyeongnam 641-831, Korea
***Materials Processing Division, Korea Institute of Materials Science, 66, Sangnam-dong, Changwon, Gyeongnam 641-831, Korea
****Department of Chemistry, Sungkyunkwan University, Suwon 440-746, Korea
(*Received 2 January 2013 • accepted 24 February 2013*)

Abstract−We have introduced water-in-oil emulsion systems to generate confining geometries for the self-organization of monodisperse silica nanospheres as building block particles. Then, through the slow evaporation of emulsion phases by heating, these nanospheres were packed into structural colloids such as raspberry-shaped micro-particles. The suspension of colloidal clusters was deposited onto glass substrate followed by surface modification of fluorine-containing silane coupling agent to produce superhydrophobic surface with dual scale roughness. Similar self-assembly approach was employed to fabricate macroporous micro-particles from composite micro-particles of polystyrene microspheres and antimony-doped tin oxide nanoparticles by calcination. After deposition of the porous particles and fluorine treatment with silane coupling agent, superhydrophobic surfaces which have potential applications such as self-cleaning property could be obtained with contact angle of water larger than 150°.

Key words: Silica Supraparticles, Self-assembly, Superhydrophobic Coatings

INTRODUCTION

Over the past few decades, colloidal soft matters have been studied extensively in the field of self-assembled colloidal structures for versatile applications such as photonic band gap materials, colloidal lithography, and porous supports [1-6]. In this context, a terminology such as *structured colloids* has been developed to describe the colloidal dispersion with regular complex structures and specific chemical compositions in the particulate system [7]. So far, various types of structured colloids have been synthesized via colloidal self-assemblies or chemical reaction routes for academic studies as well as practical uses [8-12]. Among them, the self-organization of building block particles inside confining geometries can be advantageous to fabricate structured colloids since further chemical reaction is not required during the assembling step and the physical organization process may lead to complex colloidal architectures to tune the final morphologies of colloidal dispersion.

Recently, emulsion-assisted approaches have been developed to fabricate spherical assemblies of colloidal particles or colloidal clusters using confining geometries of droplets [13-15]. As pioneering researches, Velev et al. developed a facile method for preparing spherical colloidal crystals of monodisperse nanospheres based on encapsulation of the building block particles in emulsion droplets and the droplet evaporation [16-18]. These emulsion-assisted approaches can be also expanded to the fabrication of the macroporous particles using sacrificial templates of organic beads to form macro-voids for various scientific and engineering researches such as separation medium, adsorption supports, catalytic materials, and light scatterers [19-22].

Lotus effect has been studied for functional water-repelling coatings since a superhydrophobic property is crucial for automobile industries, clothing, etc. For these purposes, two types of fabrication routes for nanostructures on substrates have been developed such as (1) top-down lithographic technologies and (2) bottom-up deposition or growth of nano-materials [23-25]. In this study, the bottom-up approach will be disclosed as a facile route to use structured colloids such as supraparticles or macroporous micro-particles for the fabrication of self-cleaning, superhydrophobic surfaces. Despite many advances for nature-inspired, water-repelling surfaces, the simple synthesis and use of structured colloids as coating materials has not been studied extensively, though this approach can provide microstructures with multiple length scales to the films which can enhance hydrophobic properties. For instance, raspberry-shaped particles have been synthesized by coating organic microspheres with smaller inorganic particles for the formation of surface protrusions to induce multiple length scales in structured colloids [26,27]. However, the synthesis protocol of these hybrid colloids is quite complicated since it requires the separate synthesis of organic/inorganic particles as well as the chemical reaction to form hybrid particles. Thus, it is still challenging to develop a fabrication method of structured colloids with simple routes for superhydrophobic surfaces.

We have synthesized two types of structured colloids such as supraparticles and macroporous micro-particles by evaporation-induced self-assembly. Specifically, for supraparticles of silica nanospheres, water-in-oil emulsions were prepared by shear-induced emulsification process, in which uniform silica particles were encapsulated. Then, controlled aggregation of the silica nanospheres inside emul-

†To whom correspondence should be addressed.
E-mail: yscho78@kpu.ac.kr, yscho78@gmail.com

sion droplets was induced during slow evaporation of the water droplets. For the fabrication of macroporous micro-particles, polystyrene microspheres were encapsulated with ATO (antimony-doped tin oxide) nanoparticles inside water droplets and evaporation of the droplet resulted in the formation of composite micro-particles. Then, macroporous micro-particles were obtained by burning out the organic microspheres, leaving behind porous inorganic structures. Additionally, the supraparticles and macroporous micro-particles were deposited on glass substrate, and surface treatment was performed using fluorine-containing silane coupling agent to impose water-repelling property for the fabrication of superhydrophobic surfaces.

EXPERIMENTAL

1. Materials

Tetraethylorthosilicate (TEOS, 99%, Aldrich) and ammonium hydroxide (NH_4OH, 28%, Aldrich) were used as silica precursor and basic catalyst to synthesize monodisperse silica nanospheres by modified Stober method. HPLC grade ethanol was purchased from Sigma-Aldrich. For the fabrication of colloidal aggregates of silica nanospheres, hexadecane as continuous phase and hypermer 2296 as emulsion stabilizer were purchased from Sigma-Aldrich and Croda inc., respectively. The commercial suspension of polystyrene microspheres (1 μm in diameter) and ATO (antimony-doped tin oxide) nano-colloid was obtained from Polyscience and Sukgyung AT Co. Ltd., respectively, for the synthesis of macroporous ATO micro-particles. De-ionized water was obtained using Pure Water System (Human Power, Scholar). Surface modification of coating films composed of structured colloids was performed using (heptadecafluoro-1,1,2,2,-tetrahydrodecyl) triethoxysilane (HDFTHDTES, 97%, Aldrich) and methanol (99.5%, Samchun Chemicals).

2. The Synthesis of Monodisperse Silica Nanospheres

Monodisperse silica nanospheres with 250, 410, and 520 nm in diameter were synthesized by modified Stober method using TEOS and ammonia as silicon source and catalyst, respectively. Mono-sized silica nanospheres with 750 nm in diameter were fabricated by seeded growth method. The detailed synthesis conditions can be found in our previous report [28].

3. The Evaporation-driven Self-assembly of Silica Nanospheres Inside Water-in-oil Emulsions

To synthesize self-organized silica aggregates, aqueous suspension of silica nanospheres (2 ml, 3.6-4 wt%) was mixed with hexadecane solution containing hypermer 2296 (0.3 wt%, 16 ml), followed by emulsification via mechanical shearing using homogenizer at 8,000 rpm for 40 seconds and 10,000 rpm for 20 seconds. The obtained complex fluid system composed of water droplets containing silica nanospheres was self-assembled after evaporation of water molecules by heating at 90 °C for 50 minutes and 100 °C for 10 minutes. The silica nanospheres assembled into silica aggregates were sedimented under gravity and washed with hexane followed by drying at room temperature. The silica clusters were resuspended in water medium by vortex mixing and mild sonication for 20 seconds.

4. The Fabrication of ATO Microspheres and Macroporous ATO Micro-particles from Water-in-oil Emulsions

For the synthesis of ATO (antimony-doped tin oxide) microspheres, aqueous dispersion of ATO nanoparticles purchased from Sukgyung AT Co. Ltd was diluted with de-ionized water to obtain 4 wt% of ATO dispersion. 1 ml of this mixture was dropped onto 8 ml of hexadecane with 0.3 wt% of emulsifier, Hypermer 2296, followed by the mechanical agitation at 8,000 rpm for 40 seconds and 10,000 rpm for 20 seconds using homogenizer (PRO 200, Pro Scientific Inc.) to obtain the water droplets containing ATO nanoparticles. For the self-assembly of ATO nanoparticles into spherical morphologies, the emulsion droplets were slowly evaporated by microwave heating to remove water molecules selectively. During the emulsion evaporation and shrinkage, ATO nano-colloid was self-assembled into ATO microspheres suspended in hexadecane. After sedimentation of ATO microspheres, the flocculated particles were washed with hexane and dried at room temperature, followed by redispersion in water medium.

For the synthesis of macroporous ATO (antimony-doped tin oxide) micro-particles, aqueous dispersion of ATO nanoparticles purchased from Sukgyung AT Co. Ltd. was diluted with de-ionized water to obtain 0.6 wt% of ATO colloid. This colloidal dispersion was mixed with amidine-coated polystyrene (PS) microspheres (Invitrogen, 2.6 wt%, 1 μm in diameter) in 1 : 1 volume ratio. 1 ml of this mixture was dropped onto 8 ml of hexadecane with 0.3 wt% of emulsifier, Hypermer 2296, followed by the mechanical agitation at 8,000 rpm for 40 seconds and 10,000 rpm for 20 seconds using a homogenizer (PRO 200, Pro Scientific Inc.) to obtain the aqueous emulsion droplets containing PS microspheres and ATO nanoparticles. For the self-organization of PS beads and ATO nanoparticles, the water droplets were selectively evaporated by using a microwave oven. During the emulsion evaporation and shrinkage, PS microspheres and ATO nano-colloids were self-organized into composite micro-particles. Calcination process at 500 °C for 5 hours using box furnace (EM Tech, Korea) was performed to remove organic PS particles from the composite micro-particles to obtain porous ATO micro-particles. The heating rate was maintained as 1 °C/min.

5. Film Generation Using Structured Colloids Composed of Silica Nanospheres or ATO Nano-colloid

The aqueous dispersion of silica aggregates was dropped onto glass substrate and water medium evaporated at room temperature. For surface modification of silica clusters on glass substrate, the coating film was immersed into methanol solution containing (heptadecafluoro-1,1,2,2,-tetrahydrodecyl) triethoxysilane (HDFTHDTES) for 3 hours to prepare superhydrophobic surfaces.

The aqueous dispersion of the composite micro-particles composed of PS microspheres and ATO nanoparticles was dropped onto a cover glass followed by calcination at 500 °C to fabricate porous ATO film on glass. To prepare superhydrophobic surface, the porous ATO film was immersed into methanol solution containing HDFTHDTES for 3 hours to modify the porous surface with the fluorine-containing molecules. Similarly, an aqueous dispersion of ATO microspheres was dropped onto glass substrate followed by evaporation of water at room temperature. The surface of ATO micro-particles on glass was modified using HDFTHDTES for 3 hours for the attachment of fluorine-containing molecules.

6. Characterizations

The morphologies of the colloidal aggregates composed of silica nanospheres were observed using field emission scanning electron microscope (FE-SEM, Hitachi-S4700). ATO nanoparticles were observed by transmission electron microscope (JEOL, JEM-2010) and size distribution of the ATO nano-colloids was obtained using

(Delsa™, Nano, LS13320). The contact angle of water droplet on porous surface was measured using contact angle measurement system (Erma inc., model G-1).

RESULTS AND DISCUSSION

The fabrication process of structured colloids such as silica supraparticles is illustrated schematically in Fig. 1. Monodisperse silica nanospheres can be encapsulated inside water droplets after the emulsification by mechanical agitation of two immiscible fluids such as aqueous suspension of silica particles and hexadecane with emulsion stabilizer using homogenizer. During heating this complex fluid system, the evaporation of water from emulsion droplets induces huge capillary force due to the shrinkage of the emulsions, and the

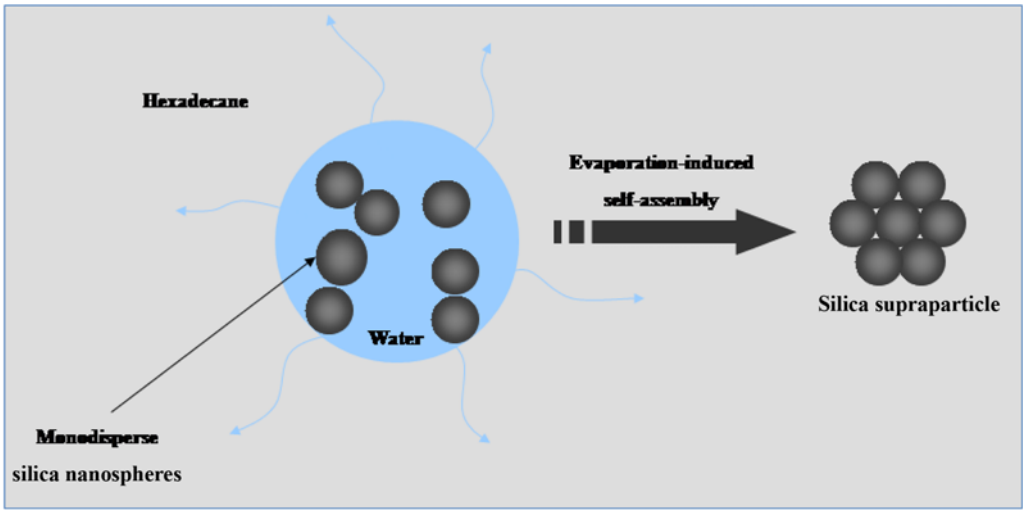

Fig. 1. Schematic of water-in-oil emulsion droplet containing silica nanospheres. After evaporation-driven self-assembly, the nanospheres can be self-organized into silica supraparticles with raspberry shape.

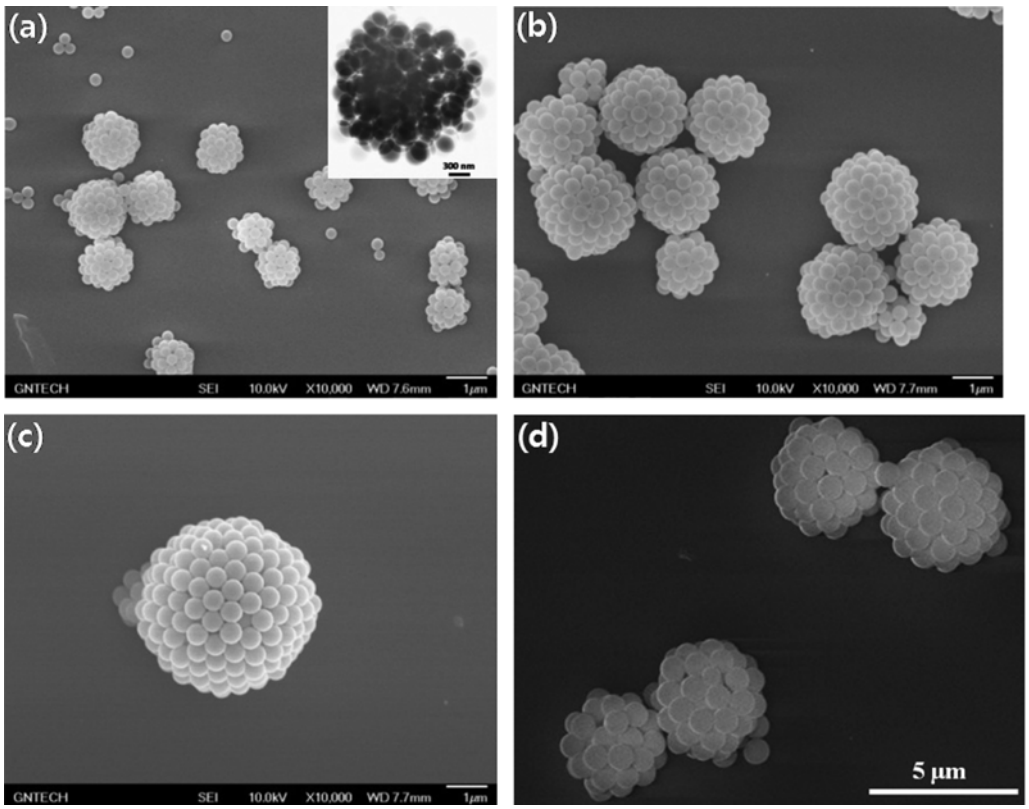

Fig. 2. SEM image of silica supraparticles fabricated using silica nanospheres with (a) 250 nm, (b) 410 nm, (c) 520 nm, and (d) 750 nm in diameter. Scale bars indicate 1 μm for (a) to (c), and 5 μm to (d). The inset of Fig. 2(a) shows the TEM image of silica supraparticles fabricated using 250-nm silica nanospheres. Scale bar in this TEM image is 300 nm.

inward capillary pressure pulls the silica nanospheres together causing the self-assembly of silica nanospheres. As a result, silica supraparticles can be fabricated after the self-organization process.

We used silica nanospheres with 250, 410, 520, and 750 nm as building block particles for the fabrication of silica supraparticles according to the self-assembly strategy shown in Fig. 1. Fig. 2(a) to 2(d) contains the resultant SEM images of silica supraparticles assembled with silica nanospheres having 250, 410, 520, and 750 nm in diameter, respectively. The morphology of each supraparticle resembles raspberry shape and spherical aggregates of silica nanospheres with various size ranges could be successfully prepared by emulsion droplets as confining geometries for self-organization process. The inset in Fig. 2(a) shows the TEM image of silica supraparticles fabricated using 250-nm silica nanospheres, indicating that the two-dimensional projection of the raspberry shaped particles composed of silica building block particles can be viewed by TEM observation.

Silica supraparticles shown in the SEM images of Fig. 2(a) to 2(d) were deposited on glass substrate by drying the suspension of the supraparticles at room temperature. After the coating step, the films were immersed in the methanol solution with fluorine-containing silane coupling agent, (heptadecafluoro-1,1, 2,2,-tetrahydrodecyl) triethoxysilane (HDFTHDTES, 1 vol%) for 3 hours to prepare superhydrophobic surfaces. Three ethoxy groups of HDFTHDTES can react with the surface hydroxyl groups of silica supraparticles by alcoholysis reaction, and the anchoring group containing fluorine atoms can increase the hydrophobicity of the coating film [29,30]. Since the original silica supraparticles are coated with hydroxyl groups, the covalent binding of HDFTHDTS on the surface of the supraparticles can be formed due to the reaction between the hydroxyl groups of silica particles and the ethoxy groups of the silane coupling agent via the following scheme [31]:

$$\equiv Si\text{-}OH + (EtO)_3\text{-}Si\text{-}X \rightarrow EtOH + \equiv Si\text{-}O\text{-}Si(OEt)_2X$$

Here, X represents the functional groups of HDFTHDTS which contains hydrocarbon chain with fluorine atoms. Thus, the surface treat-

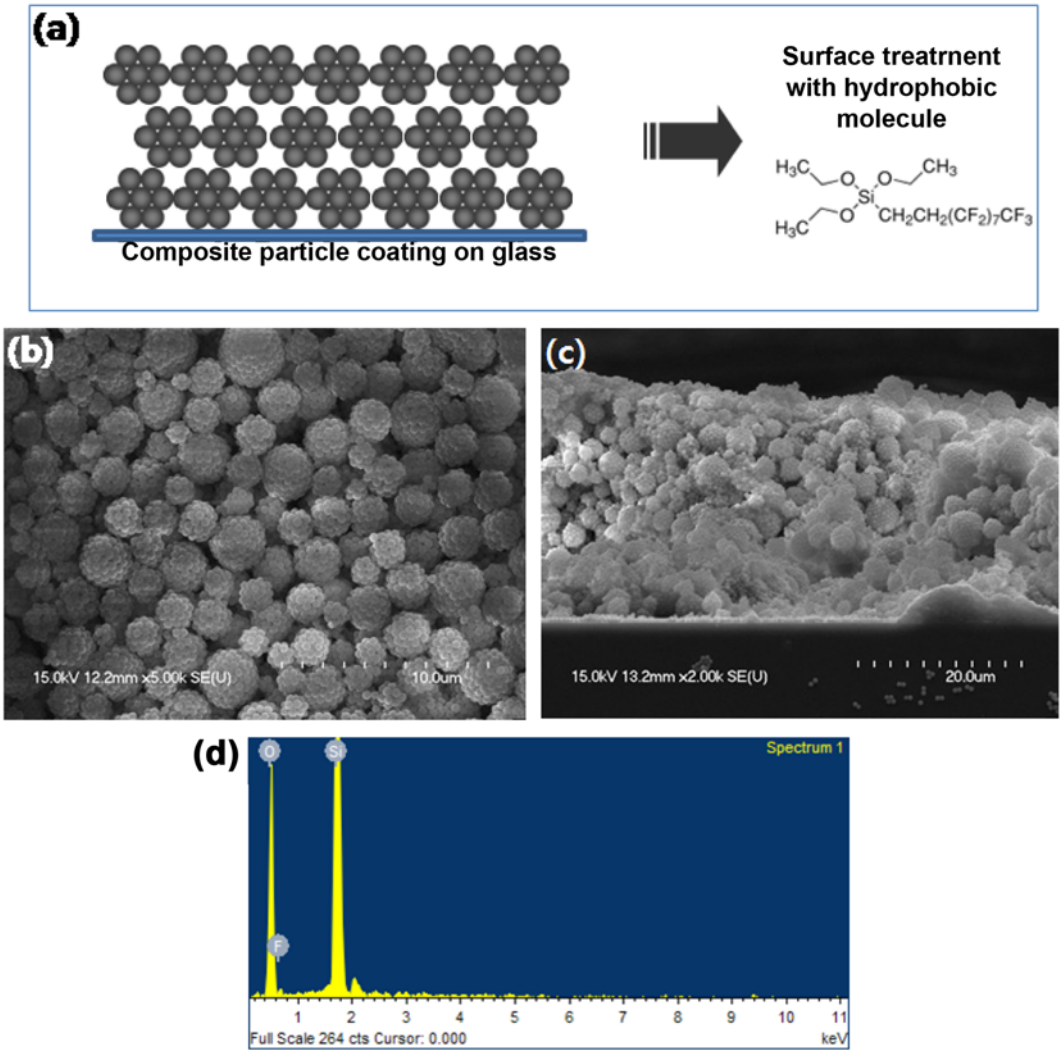

Fig. 3. (a) Schematic for the surface modification process of coating film composed of silica supraparticles for the fabrication of superhydrophobic surfaces. (b) Surface and (c) cross-sectional SEM image of coating film composed of supraparticles with 450-nm silica nanospheres. Scale bars are 10 μm and 20 μm, respectively. (d) EDS result of coating film composed of supraparticles with 450-nm silica nanospheres after fluorine coating.

ment with HDFTHDTS can change the hydrophilic nature of silica supraparticles into hydrophobic property. Fig. 3(a) contains this coating and surface treatment procedure schematically and the detailed reaction mechanism during the surface treatment procedure is omitted in the schematic figure for convenience.

The surface and cross-sectional SEM images of the coating film composed of the supraparticles with 410-nm silica nanospheres are shown in Fig. 3(b) and 3(c), respectively. From the surface SEM image, it is clear that the silica supraparticles are packed densely forming coating film with dual length scales of nanospheres and their aggregates (supraparticles), and the film thickness could be measured as about 25 μm from the cross-sectional SEM image. After the treatment of the coating film with fluorine-containing silane coupling agent, the compositions of the film were detected by EDS method, as summarized in Fig. 3(d) and Table 1, which show that 4.15 wt% of fluorine atom was recorded for superhydrophobic property.

The measured contact angles of water droplets on the coating films of silica supraparticles prepared using silica nanospheres with 250, 410, 520, and 750 nm are included in the photographs of Fig. 4(a), 4(b), 4(c), and 4(d), respectively. All samples exhibited superhydrophobicity with contact angles larger than 150°. For control experiment, the contact angle of 92.9° was measured for plain glass substrate after the surface treatment with the same silane coupling agent, as shown in the photograph of Fig. 4(e). These results indicate that silica supraparticles on glass substrate can generate superhydrophobic surfaces due to their coating structure with dual length scales such as (1) building block particles and (2) supraparticles. This superhydrophobic effect can be interpreted using the following Cassie-Baxter equation [32,33]:

$$\cos\theta_r = f(1+\cos\theta_s) - 1 \quad (1)$$

where, f, θ_s, and θ_r denote the surface area fraction of solid particles

Table 1. EDS result of coating film composed of 450-nm silica nanospheres after the treatment with fluorine-containing silane coupling agent

Element	Wt%
O	51.32
F	4.15
Si	44.53
Totals	100

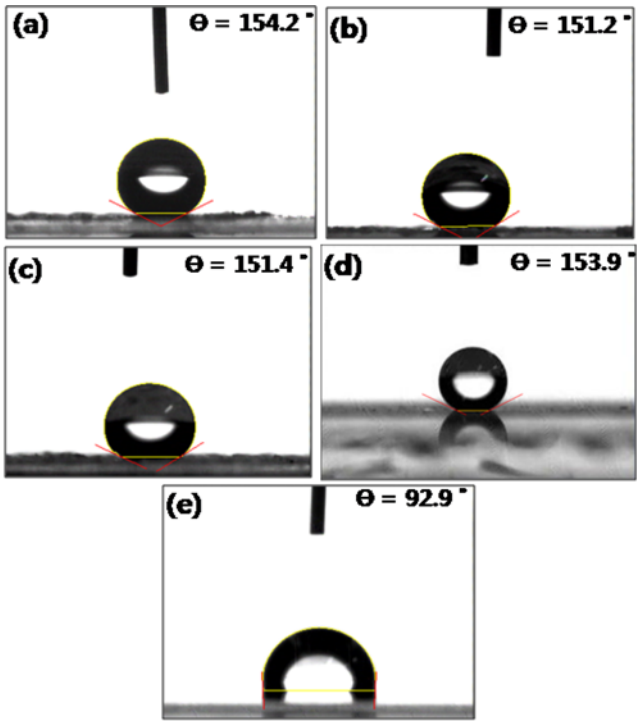

Fig. 4. Photographs of contact angle measurement result for coating film of supraparticles with constituent silica particles having (a) 250 nm, (b) 410 nm, (c) 520 nm, and (d) 750 nm in diameter. (e) contact angle measurement result of water droplet on bare glass substrate treated with the fluorine-containing silane coupling agent.

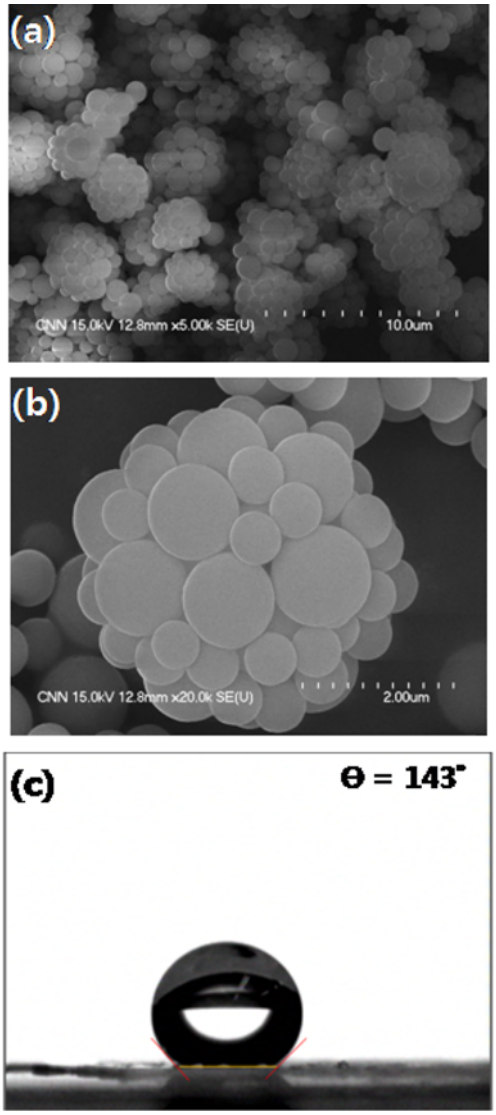

Fig. 5. (a) and (b) SEM images of silica supraparticles fabricated using bimodal silica nanospheres with 520 nm and 1 μm in diameter. Scale bar in (a) and (b) indicate 10 μm and 2 μm, respectively. (c) Contact angle measurement result of water droplet on hydrophobic film composed of silica supraparticles with bimodal constituent particles.

on glass substrate, water contact angle on flat surface, and coated surface, respectively. For instance, the surface area fraction (f) of silica materials on coated film of supraparticles with constituent silica nanospheres having 210 nm in diameter can be calculated as 10.5% using θ_s=92.9° and θ_r=154.2° from Eq. (1).

Silica supraparticles were also fabricated using bimodal dispersion of silica nanospheres with 520 nm in diameter and silica microspheres with 1 μm in diameter. Aqueous suspension of the bimodal silica particles were emulsified as dispersed phase and silica supraparticles could be synthesized by assembling the bidisperse colloids via evaporation-driven self-assembly described in the experimental section. Fig. 5(a) and 5(b) contain the SEM image of the resultant silica supraparticles of which the constituent particles have bimodal particle sizes. Using the suspension of these supraparticles, coating film was prepared by dropping and drying procedures, followed by the surface modification of the supraparticles using HDFTHDTES. Fig. 5(c) contains the photograph of the contact angle of water droplet on the surface of the coating layer of the supraparticles. The contact angle was measured as 143°, which is a smaller value compared to the films made of supraparticles fabricated using monomodal silica nanospheres shown in Fig. 3. This can be attributed to the reduced multi-scale roughness since the silica nanospheres with 520 nm in diameter are packed between the voids of the silica microspheres with 1 μm in diameter for the supraparticles shown in the SEM image of Fig. 5(a) and 5(b).

Instead of silica supraparticles, silica nanospheres with 410 nm in diameter were coated on glass substrate by vertical deposition method and the coating film was treated with HDFTHDTES for the attachment of the silane coupling agent on the coated surface, as depicted in the schematic drawing of Fig. 6(a). The microstructure on the surface of coating film is contained in the SEM image of Fig. 6(b), and the contact angle of water droplet on the coating layer is included in the photograph of Fig. 6(c). Only 92.3° of contact angle was measured, and the hydrophobicity was similar compared to the bare glass substrate treated using HDFTHDTES without silica nanospheres. Since the coating film in Fig. 6(b) has single length scale of silica nanospheres, only single scale roughness can be expected and the hydrophobicity was not enhanced unlike the superhydrophobic coatings using silica supraparticles.

Since macroporous ATO can be used for the fabrication of optically transparent and conductive electrode materials, it is possible to apply ATO nanoparticles for the synthesis of macroporous microparticles as coating materials for superhydrophobic surfaces [34]. For this purpose, we used ATO nanoparticles as starting material to synthesize macroporous ATO micro-particles by evaporation-driven self-assembly approach. Fig. 7(a) and 7(b) contain the schematic illustrations of self-assembly strategy for the fabrication of structured colloids such as microspheres and macroporous micro-particles from ATO nanoparticles, respectively. Small ATO nanoparticles can be trapped inside water emulsion droplets and they can be assembled collectively into spherical micro-particles after evaporation of water from the droplets, as displayed in Fig. 7(a). After the self-organization of the nanoparticles, ATO microspheres can be obtained since the nanoparticles can be assembled due to van der Waals force and the particles aggregate into spheres with micron sizes by surface tension induced from shrinking emulsions. On the other hand, organic templates such as PS microspheres can be added inside water droplets with small ATO nanoparticles, as illustrated schematically in Fig. 7(b). Emulsions shrink due to evaporation of water droplets by heating resulting in the formation of composite micro-particles composed of PS microspheres and ATO nanoparticles. After calcination PS microspheres can be removed and macroporous inorganic micro-particles can be fabricated.

The building block particles for the synthesis of macroporous

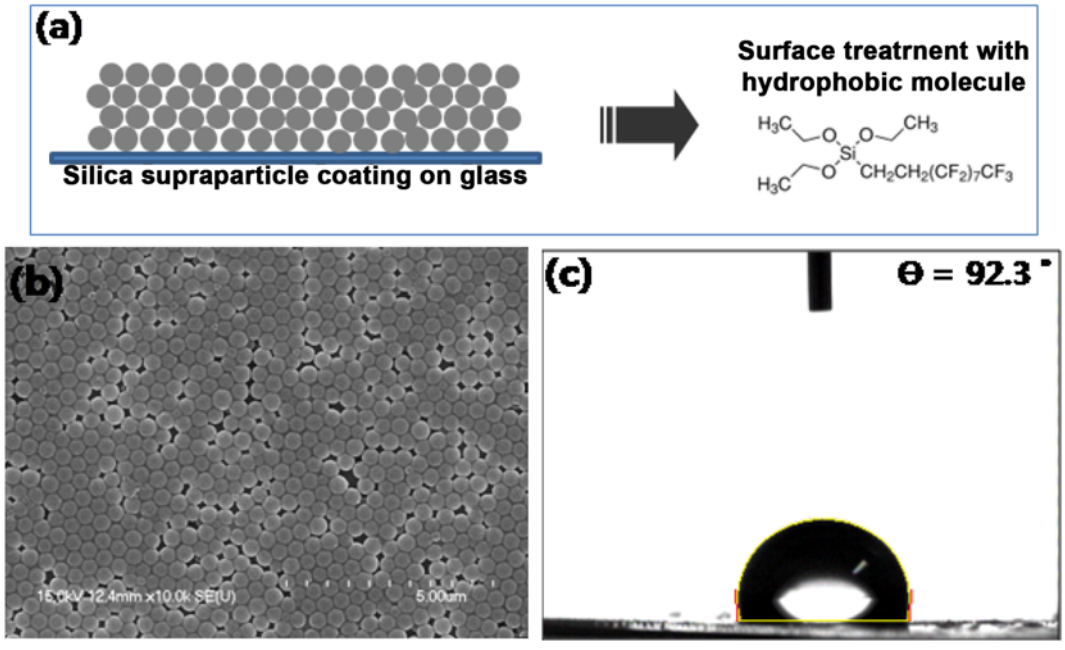

Fig. 6. (a) Schematic for the surface treatment of coating film composed of silica nanospheres. (b) SEM image of coating film composed of silica nanospheres with 410 nm in diameter. Scale bar indicates 5 μm. (c) Contact angle measurement result on the coating film composed of 410-nm silica nanospheres treated with fluorine-containing silane coupling agent.

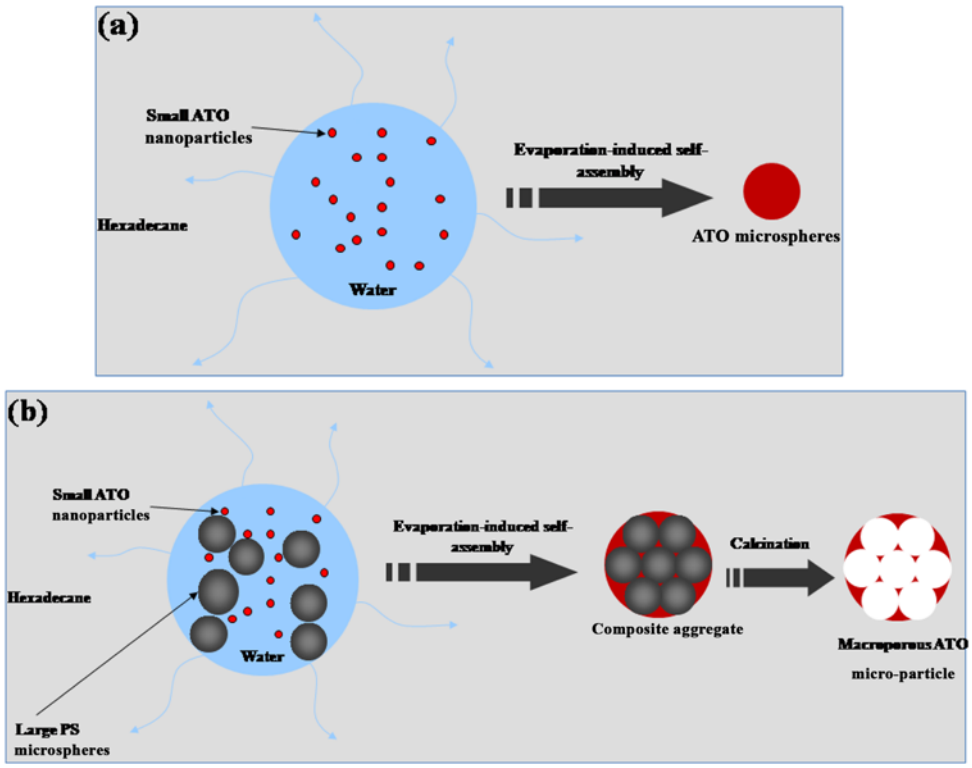

Fig. 7. (a) Schematic for the fabrication of ATO microspheres from water-in-oil emulsion droplet by evaporation-driven self-assembly (EISA). (b) Schematic representation for the fabrication of macroporous ATO micro-particles by EISA and subsequent calcination.

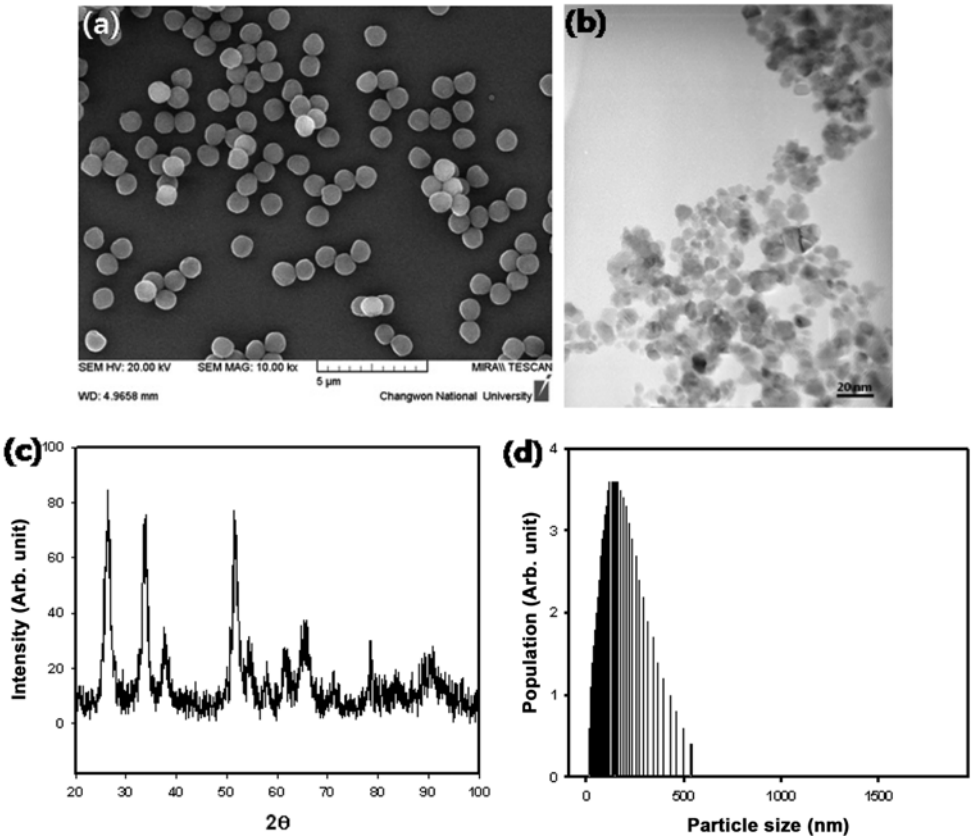

Fig. 8. (a) SEM image of polystyrene microspheres with 1 μm in diameter. Scale bar indicates 5 μm. (b) TEM image, (c) powder X-ray diffraction result, and (d) particle size distribution of ATO nano-colloids. Scale bar in (b) is 20 nm.

ATO micro-particles are displayed in Fig. 8(a) and 8(b). PS microspheres with 1 μm in diameter, which are shown in Fig. 8(a), were adopted as sacrificial templates during the fabrication of porous ATO particles. Fig. 8(b) contains the TEM image of ATO nanoparticles having primary particle size of about 20 nm. Characterization of the ATO nano-colloids was performed using powder X-ray diffraction (XRD) technique and size measurement of the colloidal dispersion. The crystallinity of ATO nanoparticles was confirmed by powder XRD analysis, which is contained in Fig. 8(c) showing the feature characteristic of SnO_2 tetragonal domain. The secondary particle size of ATO nano-colloid was measured by DLS (dynamic light scattering) system, and the measured value was about 80 nm as included in the size distribution of the colloidal dispersion in Fig. 8(d). From the histogram in Fig. 8(d), we can roughly conclude that about four primary particles form one aggregated secondary particle in the ATO colloid.

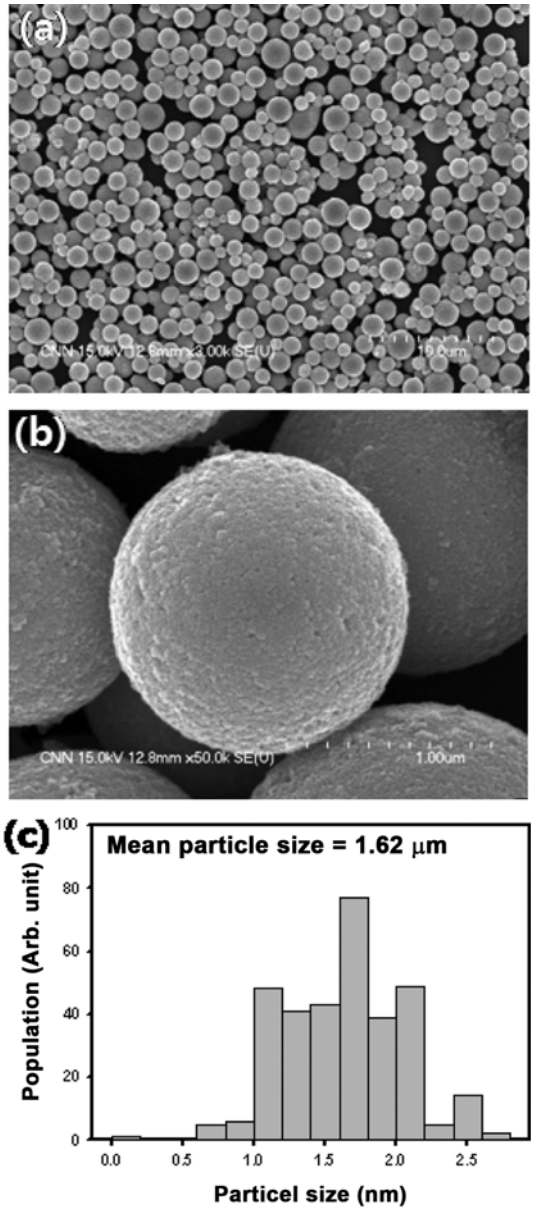

Fig. 9. (a) and (b) SEM images of ATO microspheres fabricated by EISA process. Scale bar in (a) and (b) is 10 and 1 μm, respectively. (c) Particle size distribution of ATO microspheres.

The morphology of ATO microspheres assembled with ATO nanoparticles shown in the TEM image of Fig. 8(b) is contained in the SEM image of Fig. 9(a) and 9(b). After self-organization of ATO nanoparticles, ATO microspheres with spherical shapes could be obtained since the shrinking emulsion droplet induces surface tension force which maintains the morphology of ATO micro-particles as spheres. From the magnified SEM image in Fig. 9(b), the individual ATO microsphere is comprised of small ATO nanoparticles, implying that the controlled and collective aggregation of nanoparticles resulted in the formation of spherical microstructures. The size distribution of ATO microspheres was obtained by measuring the diameters of 330 particles from the SEM image in Fig. 9(a), and the histogram is plotted in Fig. 9(c). Mean particle size was measured as 1.62 μm and the standard deviation was 0.4 μm due to the broad size distribution of the ATO microspheres. Since the ATO micro-particles were assembled from polydisperse water-in-oil emulsion droplets fabricated by mechanical shearing using homogenizer, the final ATO microspheres also exhibit polydisperse particle size, as displayed in the histogram of Fig. 9(c).

After the self-organization of ATO nanoparticles and PS microspheres inside water droplets, composite micro-particles of PS and ATO were obtained as displayed in Fig. 10(a), in which the included SEM image shows the ATO nanoparticles are packed between PS microspheres assembled due to capillary force. Calcination process was performed to fabricate macroporous ATO micro-particles from the composite micro-particles, and the resultant morphology of the porous ATO particles is contained in the SEM image of Fig. 10(b) to 10(d). Each macroporous particle possesses windows with about 500 nm in diameter, which originate from the macropores generated by the removal of PS microspheres with 1 μm in diameter, as can be observed from the SEM image of Fig. 10(b). The overall shape of the macroporous ATO micro-particles is close to spherical morphology as shown in the SEM image of Fig. 10(c), and the skeletal frameworks surrounding air voids are composed of small ATO nanoparticles with primary particle size of 20 nm in diameter, as displayed in the magnified SEM image of Fig. 10(d).

For comparison, ATO microspheres or macroporous ATO microparticles were deposited on glass substrate and the coating films were immersed in the methanol solution containing 1 vol% of fluorine-containing silane coupling agent, HDFTHDTES for 3 hours, followed by drying of the film. Fig. 11(a) illustrates this coating and surface treatment for binding of the silane coupling agent on the film surface schematically. Contact angles of water droplets were measured on the films of ATO microspheres and macroporous ATO micro-particles of which the surfaces were treated chemically with HDFTHDTES. As contained in the photograph of Fig. 11(b), the water contact angle was measured as 125.1° on the coating film composed of ATO microspheres, implying that only a slight increase of contact angle was achieved (29.2°) compared to plane glass surface treated with the fluorine-containing silane coupling agent. We can expect Wenzel state from the coating film composed of ATO microspheres in which water droplet can penetrate into the voids between the microspheres, causing relatively small contact angle [35]. Since the sliding angle of water droplet on the substrate is rela-

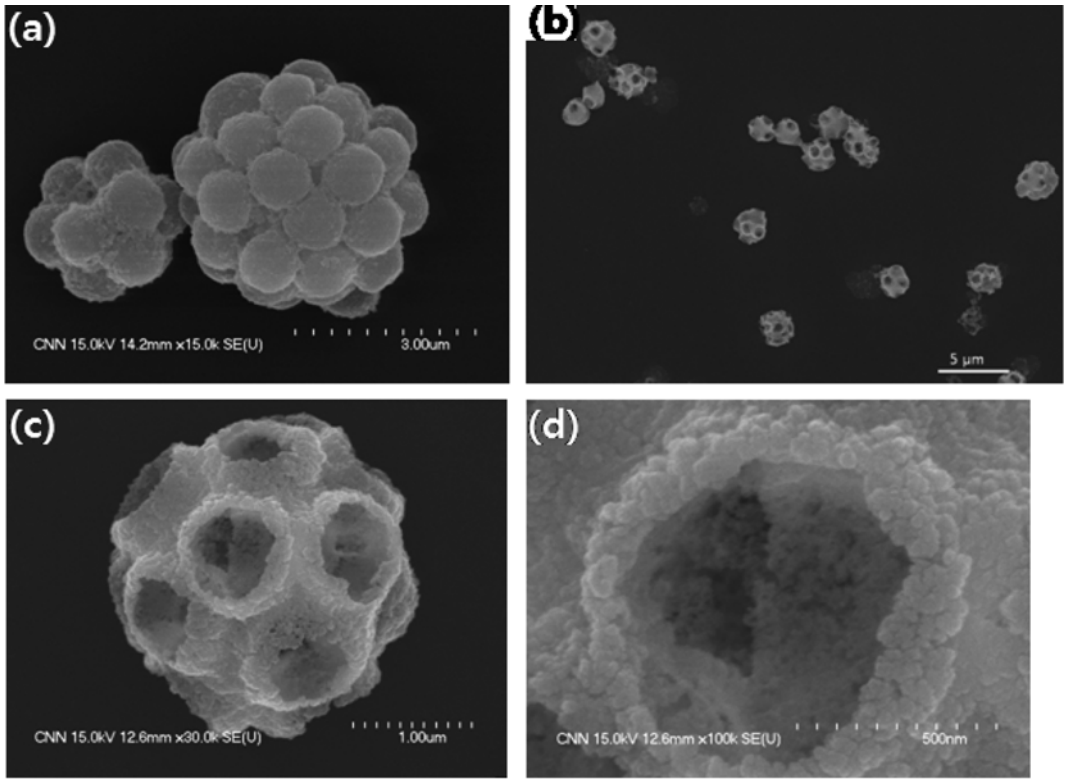

Fig. 10. (a) SEM image of composite micro-particles composed of polystyrene microspheres and ATO nanoparticles. (b) to (d) SEM images of macroporous ATO micro-particles. Scale bar in (a), (b), (c), and (d) is 3 μm, 5 μm, 1 μm, and 500 nm, respectively.

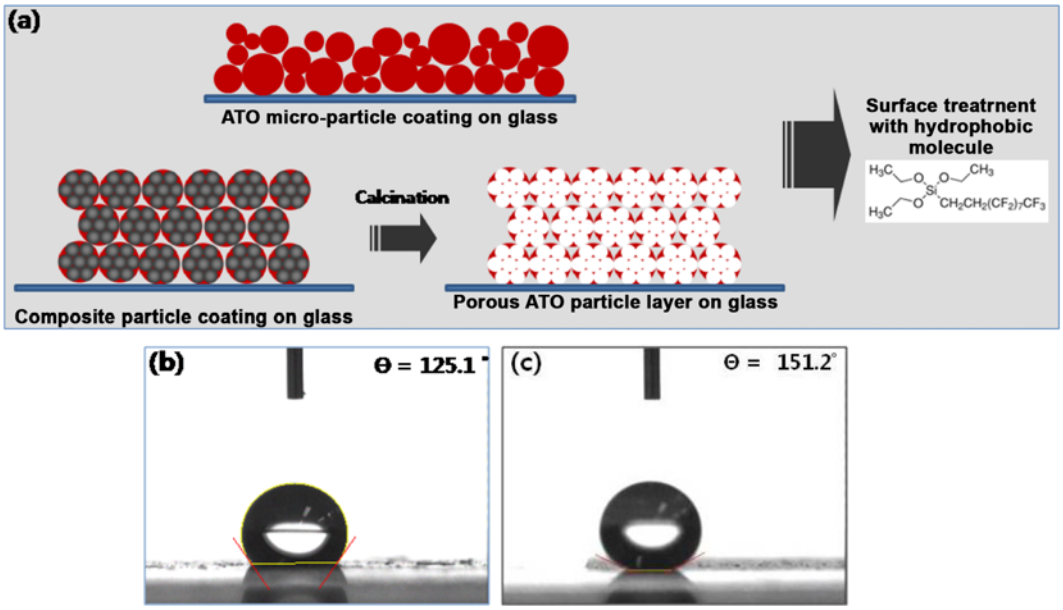

Fig. 11. (a) Schematic for the surface treatment of coating film composed of ATO microspheres or macroporous ATO micro-particles using fluorine-containing silane coupling agent. (b) and (c) contact angle of water droplet on the film composed of ATO microspheres and macroporous ATO micro-particles, respectively.

tively large for Wenzel mode, we tried to measure the sliding angle for the coating film of ATO microspheres [36]. The measurement of sliding angle of water droplet on the coating film composed of ATO microspheres was performed by using sliding angle measurement system equipped with digital angle meter shown in Fig. S1. Though we slowly inclined the coating film with water droplet on its surface just before the sliding of the droplet during the measurement, droplet pinning was observed, indicating that the water droplet is strongly adhered on the coating film, as shown in the photograph of Fig. S2. This can be explained by the formation of the capillary force after

the infiltration of the droplet between the ATO microspheres in the coating film, which confirms the Wenzel state for this case.

The roughness factor of the coating film composed of ATO microspheres can be interpreted using the following Wenzel equation [37]:

$$\cos\theta_r = r\cos\theta_s \quad (2)$$

where r, θ_r, and θ_s denote the roughness factor, water contact angle on the rough, and flat surface, respectively. For our sample, the value of r was calculated as 11.36 from Eq. (2). Since the roughness factor has been defined as the ratio between the true surface area and its horizontal projection, the value of r (11.36) for the coating film of ATO microspheres indicates that the porous surface was produced after the deposition of the microspheres [38]. For comparison, we can consider the coating film composed of square lattice of cylindrical pillar structure, in which the roughness factor r can be defined as the following equation:

$$r = 1 + \pi dh/p^2 \quad (3)$$

where, d, h, and p denote the pillar diameter, pillar height, and the pitch of the square lattice [39]. For the case of close packed microgrooves with d=20 μm, h=60 μm, and p=20 μm, the roughness factor can be easily calculated as r=10.425, which is comparable to the value of our coating film.

On the other hand, water contact angle increased drastically for the coating layer made of macroporous ATO micro-particles, which is larger than 150° (151.2°) as displayed in the photograph of Fig. 11(c). The formation of superhydrophobicity can be explained by the concept of Cassie-Baxter effect, which can be applicable to the macroporous ATO surface with multiple length scales containing air void [40,41]. For this case, the water droplet cannot penetrate the porous ATO film since air is assumed to be filled inside the porous layer, and Eq. (1) can be applicable to calculate the value f (the surface area fraction of solid particles) as 13.03% from Eq. (1).

Fig. 12(a) to 12(d) contain the time-lapsed images of rolling water droplet on superhydrophobic surface composed of macroporous ATO micro-particles after the treatment with HDFTHDTES. Since the coating film was slightly oblique, the water droplet injected from syringe impinged on the superhydrophobic surface maintaining its spherical morphology, and moved in lateral direction without spreading behavior within a short time interval. This water-repelling phenomenon is recorded and included as supporting movie file.

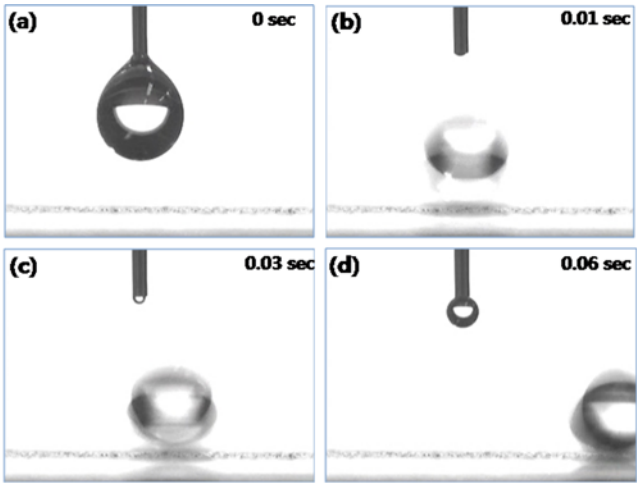

Fig. 12. (a) to (d) Time-lapsed images of rolling water droplet on superhydrophobic surface with macroporous ATO micro-particles after the treatment using fluorine-containing silane coupling agent. The movie file of the rolling water droplet is contained in the supporting information.

Table 2. Contact angles of water droplets on the coating films of supraparticles, nanospheres, and macroporous micro-particles

Film type	Water contact angle
Bare glass with F-coating*	92.9°
Silica supraparticles (silica nanosphere=250 nm)	154.2°
Silica supraparticles (silica nanosphere=410 nm)	151.2°
Silica supraparticles (silica nanosphere=520 nm)	151.4°
Silica supraparticles (silica nanosphere=750 nm)	153.9°
Silica supraparticles (silica nanosphere=520 nm, silica microspheres=1 μm)	143°
Silica nanospheres (410 nm)	92.3°
ATO microspheres	125.1°
Macroporous ATO micro-particles	151.2°

*F-coating stands for the surface treatment with fluorine-containing silane coupling agent

As summary, the contact angles of water droplets on various substrates are displayed in Table 2. Using silica supraparticles or macroporous ATO micro-particles, the coating films exhibited superhydrophobic properties with contact angles larger than 150°. A few exceptions were observed for coating films obtained by using bimodal dispersion of silica particles, possibly due to the reduction of multi-scale roughness. The film made of ATO microspheres had small contact angle such as 125.1°, in which Wenzel model is applicable.

CONCLUSIONS

Monodisperse silica nanospheres were self-organized into colloidal clusters which resemble raspberry-shaped micro-particles by evaporation-driven self-assembly inside water-in-oil emulsions. During the droplet shrinkage by heating, the silica nanospheres encapsulated inside the emulsion droplets were self-assembled into colloidal supraparticles which could be used to fabricate coating films with dual-scale roughness for the fabrication of superhydrophobic surfaces. The water-in-oil emulsion system used in this study could also provide confining geometries for the self-organization of the polymer microspheres with antimony-doped tin oxide nanoparticles, and composite structured micro-particles were obtained by evaporation-driven self-assembly process. After calcination, the resultant macroporous micro-particles could be used as inorganic frameworks to generate superhydrophobic film after surface modification with fluorine-containing silane coupling agent.

ACKNOWLEDGEMENTS

This research was supported by a grant (PGE0260) from the Eco-Innovation Project of the Korea Ministry of Environment, Creative Research Program (PNK3060) in Korea Institute of Materials Science (KIMS), and a grant from the Center for Advanced Soft Electronics under the Global Frontier Research Program of the Ministry of Education, Science and Technology, Korea.

SUPPORTING INFORMATION

Additional information as noted in the text. This information is available via the Internet at http://www.springer.com/chemistry/journal/11814.

REFERENCES

1. Y.-S. Cho, G.-R. Yi, J. H. Moon, D.-C. Kim, B.-J. Lee and S.-M. Yang, *Langmuir*, **21**, 10770 (2005).
2. H. M. Yu, A. R. Kim, J. H. Moon, J. S. Lim and K. Y. Choi, *Bull. Korean Chem. Soc*., **32**, 2178 (2011).
3. J. H. Moon, W.-S. Kim, J.-W. Ha, S. G. Jang, S.-M. Yang and J. K. Park, *Chem. Commun.*, **32**, 4107 (2005).
4. D.-G. Choi, S. G. Jang, S. Kim, E. Lee, C.-S. Han and S.-M. Yang, *Adv. Funct. Mater*., **16**, 33 (2006).
5. Y.-S. Cho, T.-Y. Kim, G.-R. Yi, Y.-K. Kim and C. J. Choi, *Bull. Korean Chem. Soc*., **33**, 159 (2012).
6. F. Iskandar, M. Abdullah and K. Okuyama, *Nano Lett*., **1**, 231 (2001).
7. S.-M. Yang, S.-H. Kim, J.-M. Lim and G.-R. Yi, *J. Mater. Chem.*, **18**, 2177 (2008).
8. A. Blaaderen, *Nature*, **439**, 545 (2006).
9. Y.-S. Cho, G.-R. Yi, J.-M. Lim, S.-H. Kim, V. N. Manoharan, D. J. Pine and S. M. Yang, *J. Am. Chem. Soc.*, **127**, 15968 (2005).
10. C. I. Zoldesi and A. Imhof, *Adv. Mater*., **17**, 924 (2005).
11. G. Lee, Y.-S. Cho, S. Park and G.-R. Yi, *Korean J. Chem. Eng.*, **28**, 1641 (2011).
12. Y.-S. Cho, S.-H. Kim and J. H. Moon, *Korean J. Chem. Eng.*, **29**, 1102 (2012).
13. S. M. Klein, V. N. Manoharan, D. J. Pine and F. F. Lang, *Langmuir*, **21**, 6669 (2010).
14. G.-R. Yi, V. N. Manoharan, S. Klein, K. R. Brzezinska, D. J. Pine, F. F. Lange and S.-M. Yang, *Adv. Mater.*, **14**, 1137 (2002).
15. V. N. Manoharan, M. T. Elsesser and D. J. Pine, *Science*, **301**, 483 (2003).
16. O. D. Velev, A. M. Lenhoff and E. W. Kaler, *Science*, **287**, 2240 (2000).
17. O. D. Velev, K. Furasawa and K. Nagayama, *Langmuir*, **12**, 2385 (1996).
18. D. M. Kuncicky, K. Bose, K. D. Costa and O. D. Velev, *Chem. Mater*., **19**, 141 (2007).
19. X. Wang, S. M. Husson, X. Qian and S. R. Wickramasinghe, *J. Membr. Sci*., **365**, 302 (2010).
20. M. Xu, D. Feng, R. Dai, H. Wu, D. Zhao and G. Zheng, *Nanoscale*, **3**, 3329 (2011).
21. A. B. D. Nandiyanto, F. Iskandar and K. Okuyama, *Chem. Eng. J*., **152**, 293 (2009).
22. J. H. Moon, Y.-S. Cho and S.-M. Yang, *Bull. Korean Chem. Soc*., **30**, 2245 (2009).
23. R. Furstner, W. Barthlott, C. Neinhuis and P. Walzel, *Langmuir*, **21**, 956 (2005).
24. Q. D. Xie, G. Q. Fan, N. Zhao, X. L. Guo, J. Xu, J. Y. Dong, L. Y. Zhang, Y. J. Zhang and C. C. Han, *Adv. Mater.*, **16**, 1830 (2004).
25. J.-M. Lim, G.-R. Yi, J. H. Moon, C.-J. Heo and S. M. Yang, *Langmuir*, **23**, 7981 (2007).
26. W. Ming, D. Wu, R. Benthem and G. With, *Nano Lett*., **5**, 2298 (2005).
27. D. Xu, M. Wang, X. Ge, M. Lam and X. Ge, *J. Mater. Chem*., **22**, 5784 (2012).
28. Y.-S. Cho, Y.-K. Kim, S.-J. Son and C.-J. Choi, *Abstracts of IEEE NMDC 2012 Conference*, 522 (2012).
29. Y.-S. Cho, G.-R. Yi, J.-J. Hong, S. H. Jang and S.-M. Yang, *Thin Solid Film*, **515**, 1864 (2006).
30. Y.-S. Cho, H.-M. Kim, J.-J. Hong, G.-R. Yi, S. H. Jang and S. M. Yang, *Colloids Surf. A*, **336**, 88 (2009).
31. K. Miyatake, O. Ohama, Y. Kawahara, A. Urano and A. Kimura, *SEI Tech. Rev.* No. 65, 21 (2007).
32. A. B. D. Cassie and S. Baxter, *Trans. Faraday Soc*., **40**, 546 (1944).
33. D. Wu, *Nature inspired superhydrophobic surfaces*, Eindhoven University Press, Eindhoven, Netherlands (2007).
34. E. Arsenault, N. Soheilnia and G. A. Ozin, *ACS Nano*, **5**, 2984 (2011).
35. E. Martines, K. Seunarine, H. Morgan, N. Gadegaard, C. D. W. Wilkinson and M. O. Riehle, *Nano Lett.*, **5**(10), 2097 (2005).
36. D. S. Kim, B.-K. Lee, J. Yeo, M. J. Choi, W. Yang and T. H. Kwon, *Microelectron. Eng.*, **86**, 1375 (2009).
37. A. V. Rao, A. B. Gurav, S. S. Latthe, R. S. Vhatkar, H. Imhai, C. Kappenstein, P. B. Wagh and S. C. Gupta, *J. Colloid Interface Sci*., **352**, 30 (2010).
38. R. N. Wenzel, *J. Phys. Chem*., **53**(9), 1466 (1949).
39. R. M. Frei, *Contact angle investigations on substrates with controlled periodic roughness: different asperity sizes and different substrate temperatures*, Semester Project, Swiss Federal Institute of Technology (EPFL), Lausanne, Switzerland (2004).
40. Y.-S. Cho, S.-Y. Choi, Y.-K. Kim and G.-R. Yi, *J. Colloid Interface Sci.*, **386**, 88 (2012).
41. Y. Li, W. Cai, B. Cao, G. Duan, F. Sun, C. Li and L. Jia, *Nanotechnology*, **17**, 238 (2006).

Supporting Informations

Fabrication of superhydrophobic surfaces using structured colloids

Young-Sang Cho*,†, Jong Woo Moon*, Dong Chan Lim, and Young Dok Kim*****

*Division of Powder and Ceramics, Korea Institute of Materials Science,
66, Sangnam-dong, Changwon, Gyeongnam 641-831, Korea
**Materials Processing Division, Korea Institute of Materials Science,
66, Sangnam-dong, Changwon, Gyeongnam 641-831, Korea
***Department of Chemistry, Sungkyunkwan University, Suwon 440-746, Korea
(*Received 2 January 2013 • accepted 24 February 2013*)

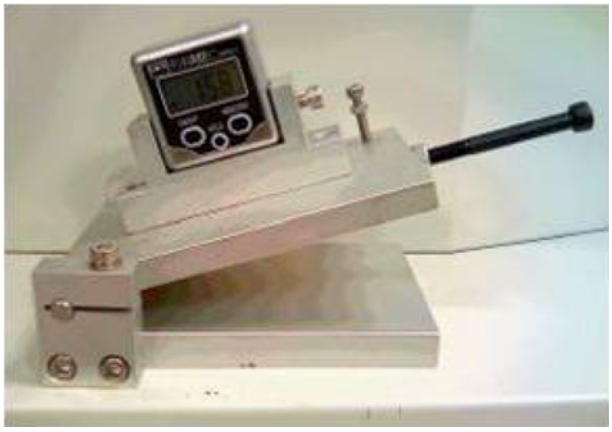

Fig. S1. Photograph of sliding angle measurement system equipped with digital angle meter.

Fig. S2. Photograph of pinning of water droplet on the coating film composed of ATO microspheres.